The flow past a freely rotating sphere

David Fabre, Joël Tchoufag, Vincenzo Citro, Flavio Giannetti, Paolo Luchini

David Fabre · Joël Tchoufag · Vincenzo Citro
Flavio Giannetti · Paolo Luchini

The flow past a freely rotating sphere

Abstract We consider the flow past a sphere held at a fixed position in a uniform incoming flow but free to rotate around a transverse axis. A steady pitchfork bifurcation is reported to take place at a threshold $Re^{\mathrm{OS}} = 206$ leading to a state with zero torque but nonzero lift. Numerical simulations allow to characterize this state up to $Re \approx 270$ and confirm that it substantially differs from the steady-state solution which exists in the wake of a fixed, non-rotating sphere beyond the threshold $Re^{\mathrm{SS}} = 212$. A weakly nonlinear analysis is carried out and is shown to successfully reproduce the results and to give substantial improvement over a previous analysis (Fabre et al. in J Fluid Mech 707:24–36, 2012). The connection between the present problem and that of a sphere in free fall following an oblique, steady (OS) path is also discussed.

Keywords Freely moving bodies · Fluid–structure interactions · Weakly nonlinear expansion

1 Introduction

Free falling and rising of particles in Newtonian fluids play an important role in many industrial and natural applications, such as the settling of sediments in lakes, buoyancy-driven bodies in the atmosphere or the dynamics of catalysts in chemical reactors. The particle motion is caused by the buoyancy force that is balanced by the hydrodynamic resistance. The resulting wake dynamics can lead to completely different regimes, such as tumbling, zigzag or steady oblique paths [1]. The mechanisms leading to path destabilization are related to intrinsic wake instabilities which induce lift and torque forces on the bodies. Yet, in general, the relation between wake instabilities around a fixed body and path instabilities around a body in free fall is not straightforward as the latter problem is fully coupled and the wake dynamics are modified by the motion of the body (as discussed for instance in Assemat et al. [2] and Auguste et al. [3]). Thus, it may be useful to consider intermediate problems in which only some degrees of freedom of the body are allowed. This is the objective of the present paper, where we will consider the flow past a sphere allowed to rotate but not to translate. In an experimental setup, this configuration may correspond, for instance, to the case of a sphere held by a thin transverse wire.

Communicated by Dr. Vassilios Theofilis.

D. Fabre
Institut de Mécanique des Fluides de Toulouse (IMFT) - Allée Camille Soula, Université de Toulouse, 31400 Toulouse, France

J. Tchoufag
Department of Mechanical Engineering, University of California, Berkeley, CA 94720, USA

V. Citro (✉) · F. Giannetti · P. Luchini
DIIN, University of Salerno, Via Giovanni Paolo II, 84084 Fisciano, SA, Italy
E-mail: vcitro@unisa.it

The case of a sphere is among the simplest and most generic geometries and has thus already made the object of a number of studies (see [4] for an up-to-date review). When the sphere is fixed and not rotating, the flow remains axisymmetric at low Reynolds numbers, but bifurcates toward a steady-state (SS) solution with a planar symmetry and nonzero lift at $Re^{\mathrm{SS}} = 212$. A subsequent Hopf bifurcation then occurs at $Re \approx 276$ leading to a periodic vortex shedding mode [5]. The case where the sphere is fixed but rotating in an imposed way was recently considered by [4]. They showed that in the presence of weak rotation, the bifurcation at Re^{SS} becomes an imperfect one. They also showed that rotation has a strong effect on the secondary Hopf bifurcation. The case of a sphere in free motion also made the object of a number of studies, both experimental [6–8] and numerical [9,10]. For Reynolds numbers in the range beyond 300, up to four unsteady regimes were discovered, but for smaller Reynolds, all studies show that the first bifurcation is toward an oblique, steady (OS) path which bears some similarity with the steady state (SS) existing for the fixed, non-rotating sphere. However, the connection between both states is not that straightforward, and Fabre et al. [11] showed that the OS state results from a bifurcation at a threshold $Re^{\mathrm{OS}} = 206$ which is different from the value $Re^{\mathrm{SS}} = 212$ for the SS state. Fabre et al. [11] also pointed out that the OS state is characterized by zero torque exerted on the sphere, so this state is also directly a valid equilibrium solution for the present problem where the sphere is free to rotate but not to translate. The study of [11] was done using an asymptotic approach which is valid under the assumption that the rotation rate is weak. However, a major drawback of this approach is that it fails in the vicinity of $Re^{\mathrm{SS}} = 212$ and beyond, while numerical and experimental results show that the OS path still exists above this value of Re.

In the present paper, we will thus investigate the case of a sphere where rotation is allowed but not translation, which is closely related to the situation discussed above. After setting the problem in Sect. 2, we will document this situation in Sect. 3, through DNS results and compare with the case where both translation and rotation are blocked. We then conduct in Sect. 4 a weakly nonlinear analysis of this problem, which will confirm that a steady bifurcation occurs for the same value Re^{OS} as for the case where both rotation and translation are allowed, and overcome the difficulties encountered in the previous study of [11]. Finally, conclusions will be provided in Sect. 5.

2 Problem definition and governing equations

The situation investigated here is sketched in Fig. 1. A sphere of radius R and density ρ_b is placed in a flow of velocity U_0 of a fluid with density ρ_{f} and viscosity ν. The problem involves two dimensionless control parameters, namely the Reynolds number $Re = U_0 R/\nu_{\mathrm{f}}$ and the body-to-fluid density ratio $\bar{\rho} = \rho_b/\rho_{\mathrm{f}}$. We formulate the problem in a fixed system of axes (x, y, z) with the unit vector $\mathbf{x}$ aligned with the incoming velocity.

In the setup considered here, the only degree of freedom is the rotation of the sphere around its center. We note Ω the angular velocity vector and decompose it over the basis as $\Omega = \Omega_x \mathbf{x} + \Omega_y \mathbf{y} + \Omega_z \mathbf{z}$.

The flow field $[\mathbf{V}, P]$ and the rotation rate Ω of the sphere are governed by the following equations:

$$\nabla \cdot \mathbf{V} = \mathbf{0}, \tag{1a}$$

$$\frac{\partial \mathbf{V}}{\partial t} + \mathbf{V} \cdot \nabla \mathbf{V} = -\nabla P + \frac{1}{Re} \nabla^2 \mathbf{V}, \tag{1b}$$

$$\bar{\rho} \frac{\pi}{60} \frac{\mathrm{d}\Omega}{\mathrm{d}t} = \mathbf{M}. \tag{1c}$$

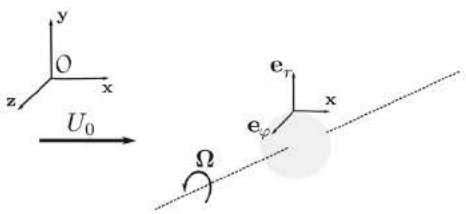

Fig. 1 Problem configuration. The sphere is free to rotate (but not to translate) around the transverse axis

These equations are coupled in two ways. First, the rotation of the sphere results in a boundary condition to be imposed for the velocity of the fluid at the surface of the sphere as $\mathbf{V} = \Omega \times \mathbf{r}$. Secondly, in Eq. (1c) the sphere responds to the torque $\mathbf{M}$ exerted by the fluid on it. The latter and the associated force $\mathbf{F}$ are given by

$$\mathbf{F} = \int_{\mathscr{S}} \mathbf{T} \cdot \mathbf{n} \mathrm{d}S \equiv F_x \mathbf{x} + F_y \mathbf{y} + F_z \mathbf{z} \tag{2a}$$

$$\mathbf{M} = \int_{\mathscr{S}} \mathbf{r} \times (\mathbf{T} \cdot \mathbf{n}) \mathrm{d}S \equiv M_x \mathbf{x} + M_y \mathbf{y} + M_z \mathbf{z}. \tag{2b}$$

where $\mathbf{r}$ denotes the position vector relative to the body center of inertia and $\mathbf{T} = -P\mathbf{I} + Re^{-1}(\nabla \mathbf{V} +^{\mathrm{T}} \nabla \mathbf{V})$ the stress tensor. Note that in the present case, the coupling only involves the torque $\mathbf{M}$ while the force $\mathbf{F}$ is not coupled to the motion of the sphere, unlike in the more general case considered in [12]. Finally, this set of equations is completed by the boundary condition $\mathbf{V} = \mathbf{U_0 x}$ for $\|\mathbf{r}\| \to \infty$.

In the following, we will be mostly interested in the characterization of steady-state solutions of the problem. According to (2b), such states imply the torque $\mathbf{M}$ exerted by the fluid on the sphere to be zero, and the interesting, non-trivial solutions are those with nonzero rotation rate Ω.

3 Numerical results

We have solved numerically the set of equations (1) using a combined finite-difference second-order immersed-boundary multigrid code which is described in detail in Citro et al. [4].

The 3D steady solutions can be obtained, in subcritical conditions, by simply integrating the time-dependent equations (1) over a sufficiently long time interval. However, since in the present paper we consider also supercritical conditions, we use a stabilization algorithm to obtain directly the steady solution. The method is based on the minimization of the residual norm at each integration step. It gives us steady-state solutions even in the case where they are temporally unstable. The method is briefly described in Citro et al. [13] and was also used in Citro et al. [4] for the case where the rotation rate of the sphere is imposed. Adaptation to the freely rotating case simply adds the dynamical equation (1c) to the latter problem, and adaptation of the method to this case is straightforward.

We discretized the computational domain using structured grids that are symmetric with respect to the plane $z = 0$. These meshes are clustered near the sphere surface. We performed several numerical tests showing the effect of the resolution and domain length on the flow field characteristics to validate our code. In particular, as an example, we present here the convergence of the lift coefficient C_{L} as the grid is refined. Tables 1 and 2 show variations of C_{L} less than 0.5 % when increasing the number of points and/or lengthening the domain. The value of the lift coefficient, computed for the same Reynolds number by the Spectral element solver $Nek5000$,

Table 1 Meshes used in the present study to validate our numerical setup

Mesh	Parameters				
	L_x	L_y	L_z	N_x	$N_y = N_z$
$\mathbb{M}1$	35	18	18	288	240
$\mathbb{M}2$	38	21	21	364	320
$\mathbb{M}3$	38	21	21	482	380

N_x, N_y, N_z are the number of points used to discretize the computational domain in x-, y- and z-direction, respectively

Table 2 Influence of the spatial grid resolution and domain extension on the lift coefficient C_{L} at $Re = 260$

Mesh	C_{L}	Method
$\mathbb{M}1$	0.06490	IBM
$\mathbb{M}2$	0.06589	IBM
$\mathbb{M}3$	0.06608	IBM
–	0.06592	$Nek5000$

We compare also the results obtained by using the immersed-boundary multigrid (IBM) code and lift coefficient provided by $Nek5000$

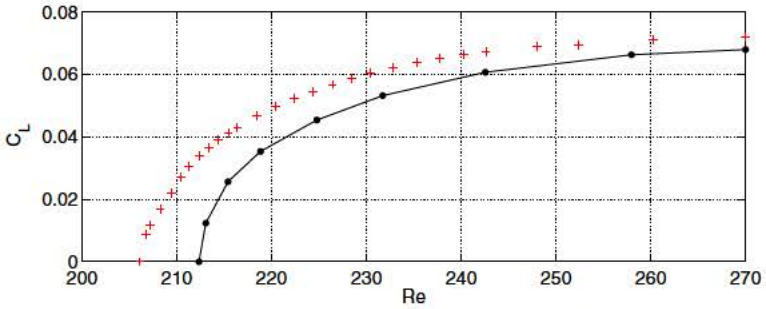

Fig. 2 Lift coefficient C_L as function of Re for both fixed (*dots*) and freely (*plus symbol*) rotating sphere

is also reported as validation. The numerical approach adopted in this code is described in Tammisola et al. [14] and Lashgari et al. [15].

For $Re < Re^{\mathrm{OS}} = 206$, only axisymmetric solutions with zero rotation rate and only a drag force are found. Above this threshold, depending upon initial conditions the numerical method yields either an axisymmetric solution or a set non-axisymmetric solutions with nonzero rotation rate around an axis perpendicular to the incoming flow and a nonzero lift. Because of the rotational symmetry, all orientations of axis of rotation are theoretically allowed. In the sequel, we will assume a rotation rate Ω_z around the **z** axis. Accordingly, the lift will be exerted along the **y** axis, and we define the lift coefficient as $C_\mathrm{L} = 2F_y/(\pi\rho R^2)$.

Figure 2 characterizes the rotating solution through a plot of the lift coefficient as function of the Reynolds number up to $Re = 240$. The plot is characteristic of a pitchfork bifurcation occurring for $Re = 206$. In the same figure, we plot the lift coefficient in the related problem of a non-rotating sphere, with data taken from figure 3 of Citro et al. [4]. As expected in this case, the bifurcation occurs for $Re^{\mathrm{SS}} = 212$ and the two curves notably differ up to $Re \approx 230$. For higher values of the Reynolds number, the two curves tend to approach each other, suggesting that allowing rotation has only a mild effect on the structure of the flow.

4 Asymptotic expansion of the coupled fluid–sphere system

4.1 Analysis

Using notations similar to those used in [12] of the study of objects in free fall, the solution of Eq. (1) may be considered as a state vector $\mathbf{Q} = \left[\mathbf{Q}^f, \mathbf{Q}^b\right]^{\mathrm{T}}$, where $\mathbf{Q}^f = [\mathbf{V}(\mathbf{r}, t), P(\mathbf{r}, t)]^{\mathrm{T}}$ describes the fluid local velocity and pressure and $\mathbf{Q}^b = \Omega(t)$ gathers the degrees of freedom associated with the body (here only the rotational velocity).

Thus, we investigate the vicinity of $Re_c = Re^{\mathrm{OS}}$ by defining a small parameter $\epsilon = \sqrt{Re - Re_c}/Re_c$. To this aim, following [16,17], we introduce a multiscale time expansion procedure with a fast time scale t and a slow time scale $\tau = \epsilon^2 t$ so as to expand this solution in the form:

$$\mathbf{Q} = \mathbf{Q_0} + \epsilon\mathbf{Q_1}(t, \tau) + \epsilon^2\mathbf{Q_2}(t, \tau) + \epsilon^3\mathbf{Q_3}(t, \tau) + \cdots \tag{3}$$

Injecting these expansions in the system of governing equations (1) yields a nonlinear problem at zeroth order and a linear problem at each order ϵ^j for $j \geq 1$. The details are very similar to those given in [12], except that the component $\mathbf{Q}^b$ of the state vector contains only the rotation and that the expansion is done in terms of the Reynolds number, not the Archimedes number. We refer the reader to the supplemental material in [12] for the detailed expressions. These problems are solved for increasing j, using the finite element solver FreeFem++ [18]. The numerical details regarding mesh refinement, polynomial interpolation of velocity and pressure fields, etc. can be found in [19].

The base state $\mathbf{Q_0}$ corresponds to the steady, vertical fall or rise with an axisymmetric flow field and is computed using an iterative Newton method as described in [16]. At order ϵ, $\mathbf{q_1}$ is the solution of the linear stability problem which is solved as in [19]. Taking advantage of the body axisymmetry, we express the fluid velocity and pressure fields in the body frame using cylindrical coordinates (x, r, φ) and seek this solution as a superposition of eigenmodes of the form

$$\mathbf{Q}_m = \left[\hat{\mathbf{q}}^f_m(x, r)\mathrm{e}^{\mathrm{i}m\varphi}, \hat{\mathbf{q}}^b_m\right]^{\mathrm{T}} \mathrm{e}^{\lambda t}$$

where m is the azimuthal wavenumber and $\lambda = \lambda_r + \mathrm{i}\lambda_i$ is the complex eigenvalue. The generalized eigenproblem to be solved at this order can be recast in the matrix form:

$$\lambda \mathscr{B}\mathbf{Q}_1 + \mathscr{A}(\mathbf{Q}_0)\mathbf{Q}_1 = \mathbf{0}.$$

The solutions of this problem have to be examined for each value of the azimuthal wavenumber. The case $m = 0$ corresponds to axisymmetric modes, and symmetry considerations show that the angular velocity component of the eigenmodes is in the axial direction, i.e., $\hat{\mathbf{q}}_m^b \equiv \hat{\omega}_0 \mathbf{x}$. It is found that all these modes are stable and that the least damped one is a non-oscillating one ($\lambda_i = 0$) corresponding to a motion where the sphere initially spins around the axial axis and slows down due to friction. This mode also exists in the case of a freely falling disk and was analyzed in appendix C of Tchoufag et al. [19]. In this reference, it was called the back-to-zero-rotation mode (BZR). A mode with $|m| \geq 2$ does not exert any torque on the sphere and hence is identical to those of the non-rotating ($\hat{\mathbf{q}}_m^b = \mathbf{0}$). Moreover, these modes are also found to be always stable in the range of Reynolds considered.

Hence, the most interesting case corresponds to azimuthal wavenumbers $m = \pm 1$, and as for the fixed, non-rotating sphere, a Pitchfork bifurcation associated with a steady mode ($\lambda_r = \lambda_i = 0$) is detected for $Re = Re^{\mathrm{OS}} = 206$. Following the assumption made by Fabre et al. [11], we consider these two modes adequate to quantitatively describe the characteristics of the nonlinear oblique motion of the sphere for $Re > Re_c$. Hence, restricting the following analysis to these modes, the general $O(\epsilon)$ solution at the threshold ($\lambda_r = 0$) may be expressed in the form

$$\mathbf{Q_1} = \hat{A}(\tau)\left[\hat{\mathbf{q}}_1^f(x, r)\mathrm{e}^{\mathrm{i}\varphi}, \hat{\mathbf{q}}_1^b\right]^{\mathrm{T}} + \text{c.c.}, \tag{4}$$

where $\hat{A}(\tau)$ is the $O(\epsilon)$ complex amplitude of the global mode and c.c. stands for the complex conjugate quantities, which shall be marked by a * symbol hereafter. Note that since the global mode $m = 1$ is real, its complex conjugate directly corresponds to the mode $m = -1$. Therefore, there is no need to distinguish between two amplitudes $\hat{A}^+ = A$ and $\hat{A}^- = A^*$ since the latter is completely determined once the former is.

Due to symmetry considerations (see [19]), the component of the $m = 1$ eigenmode corresponding to the rotation of the body can be written as $\hat{\mathbf{q}}_1^b = \frac{\hat{\omega}_+}{2}(\mathbf{z} + \mathrm{i}\mathbf{y})$, so the orientation of the rotation axis is given by the argument of $A\hat{\omega}_+$. We choose to normalize the eigenmode as $\hat{\omega}_+ = 1$, so that the norm of A directly gives the rotation rate. Moreover, a real A will correspond to rotation around the $\mathbf{z}$ axis (and lift along the $\mathbf{y}$ axis), while an imaginary A will correspond to rotation around the $\mathbf{y}$ axis (and lift along the $\mathbf{z}$ axis).

Terms of order ϵ^2 and ϵ^3 are the solution of linear inhomogeneous problems arising from the expansion of (1) at the corresponding order. Details about the mathematical structure of these problems and the numerical procedure used to solve them are given in the Supplemental Material in [12] where the weakly nonlinear analysis has been performed for the more general case of an unsteady mode. It suffices here to say that at order ϵ^2, the flow is modified by higher-order harmonics which obey the inhomogeneous linear system of equations

$$\partial_t \mathscr{B}\mathbf{Q_2} + \mathscr{A}(\mathbf{Q_0})\mathbf{Q_2} = \mathbf{F_2}(\mathbf{Q_0}, \mathbf{Q_1}).$$

The forcing term $\mathbf{F_2}$ on the right-hand side is made of three independent terms expressing the effect of a small variation of Re on the base flow and the interaction of one mode ($\mathbf{Q_A}$ + c.c.) with itself and its c.c. Using the linear superposition principle, we solve this inhomogeneous equation for each contribution to the forcing. The ϵ^2-order solution then reads $\mathbf{Q_2} = \hat{\mathbf{Q}}_{\delta_{Re}} + |A|^2\hat{\mathbf{Q}}_{AA^*} + (A^2\hat{\mathbf{Q}}_{AA}\mathrm{e}^{2\mathrm{i}\varphi} + \text{c.c.})$.

The problem at order ϵ^3 is also an inhomogeneous linear system, the forcing term $\mathbf{F_3}(\mathbf{Q_0}, \mathbf{Q_1}, \mathbf{Q_2})$ depending on lower-order solutions. More specifically, $\mathbf{F_3}$ contains terms of the form $\sim \mathrm{e}^{\mathrm{i}\varphi}$ which are resonant because they excite the system precisely in the direction of the unstable steady eigenmode. In order to avoid the secular responses caused by these terms, we use the Fredholm alternative and impose a compatibility condition: the resonant forcing must be orthogonal to the adjoint modes. These modes are obtained either in a continuous or in a discrete form. Here, we chose the latter option and compute the adjoint modes by solving for the eigenmodes of the hermitian of $\mathscr{A}$, the linear operator of the $O(\epsilon)$ problem. The compatibility condition then results in the following amplitude equation:

$$\frac{\mathrm{d}A}{\mathrm{d}t} = (Re - Re_c)\sigma A - \mu A|A|^2, \tag{5}$$

where $(Re - Re_c)\sigma$ is the exponential growth rate of $\mathbf{Q_1}$ in the linear regime, while μ is a real coefficient responsible for the nonlinear saturation. The numerical value of μ, contrary to that of σ, depends on the normalization of the unstable global mode. Solving for the steady solution of (5), the amplitude of the perturbation from the axisymmetric flow field reads

$$A = \pm\sqrt{\frac{(Re - Re_c)\sigma}{\mu}}. \tag{6}$$

Having in mind that the solution at order 1 has been normalized so that the angular velocity of the eigenmodes is 1, this equation directly yields a prediction for the rotation rate ω. It is noteworthy that the coefficients σ and μ appearing in the amplitude equation are actually independent upon the mass ratio $\bar{\rho}$. This point will be rediscussed in Sect. 5.

4.2 Results and discussion

As recalled in "Introduction," a previous attempt at describing the bifurcation leading to the OS state for a sphere in free fall was done in [20]. Unlike in the present approach, the analysis of [20] assumed the rotation rate ω to be small and expanded the flow around the sphere as follows:

$$\mathbf{q} = [\mathbf{V}, P] = \mathbf{q}_0 + \omega\mathbf{q}_1 + \omega^2\mathbf{q}_2 + \omega^3\mathbf{q}_3 + \cdots \tag{7}$$

Injecting this ansatz into the incompressible Navier–Stokes equations, the analysis leads to a prediction of torque exerted on the sphere under the form:

$$M = M_\omega\omega + M_{\omega^3}\omega^3 \tag{8}$$

It was thus possible to predict the existence of a solution with a nonzero rotation rate given by

$$\omega = \pm\sqrt{-\frac{M_\omega}{M_{\omega^3}}} \tag{9}$$

Note that the term M_ω becomes positive for $Re > Re^{\mathrm{OS}}$, while the term M_{ω^3} is negative in this range of Reynolds; hence, Eq. (9) also predicts a supercritical bifurcation for $Re > Re^{\mathrm{OS}}$.

The results to be discussed now correspond to the case of a rotation around the **z** axis, thus resulting in a lift force along **y**. In Fig. 3a, we compare the angular velocity ω of the OS state as predicted by the new ϵ-expansion derived in the previous paragraph (Eq. 6), as predicted by the ω-expansion of [20] (Eq. 9), and as computed numerically in Sect. 3. We also compare in Fig. 3b the associated lift forces corresponding to the three approaches. The comparison shows that, for both these quantities, the present ϵ-expansion reproduces much better the numerical results than the previous ω-expansion. In particular, the failure of the ω-expansion at $Re^{\mathrm{SS}} = 212$ is not observed anymore in the present approach.

As discussed in [11], the angle γ between the force **F** and the direction of the incoming flow **x** (given by $\tan\gamma = F_y/F_x$) directly corresponds to the slope of the path in the corresponding situation where the sphere is freely falling. This angle is plotted as function of Re in Fig. 3c). We observe again that the present ϵ-expansion reproduces much better the numerical results than the previous ω-expansion.

Note that Uhlmann and Dusek [10] studied the case of a sphere in free fall with density ratio $\bar{\rho} = 1.5$ and reported for $Re \simeq 243$ a steady oblique motion characterized by a slope $\gamma \simeq 5.2°$ and a rotation rate $\omega \simeq 0.014$. These findings thus corroborate quantitatively the results of Fig. 3.

5 Summary and discussion

In this paper, we investigated by using numerical simulations and a weakly nonlinear expansion the steady flow around a sphere placed at a fixed place in a uniform fluid flow and free to rotate around a transverse axis. A steady pitchfork bifurcation is reported to find place at a threshold $Re^{\mathrm{OS}} = 206$ leading to a state with zero torque but nonzero lift. Numerical simulations allow to characterize this state up to $Re \approx 270$ and confirm that it substantially differs from the steady-state solution which exists in the wake of a fixed sphere beyond the threshold $Re^{\mathrm{SS}} = 212$. A weakly nonlinear analysis, formally valid for $\epsilon = (Re - Re_c)/Re_c \ll 1$, is carried out and is found to reproduce accurately the results up to $Re \approx 225$, giving substantial improvement over a previous expansion conducted by [11] which was unable to predict the existence of this state beyond $Re > 212$. The connection between the present problem and that of a sphere in free fall is discussed. It is argued that the steady solution of the present problem is also an acceptable solution for the related problem

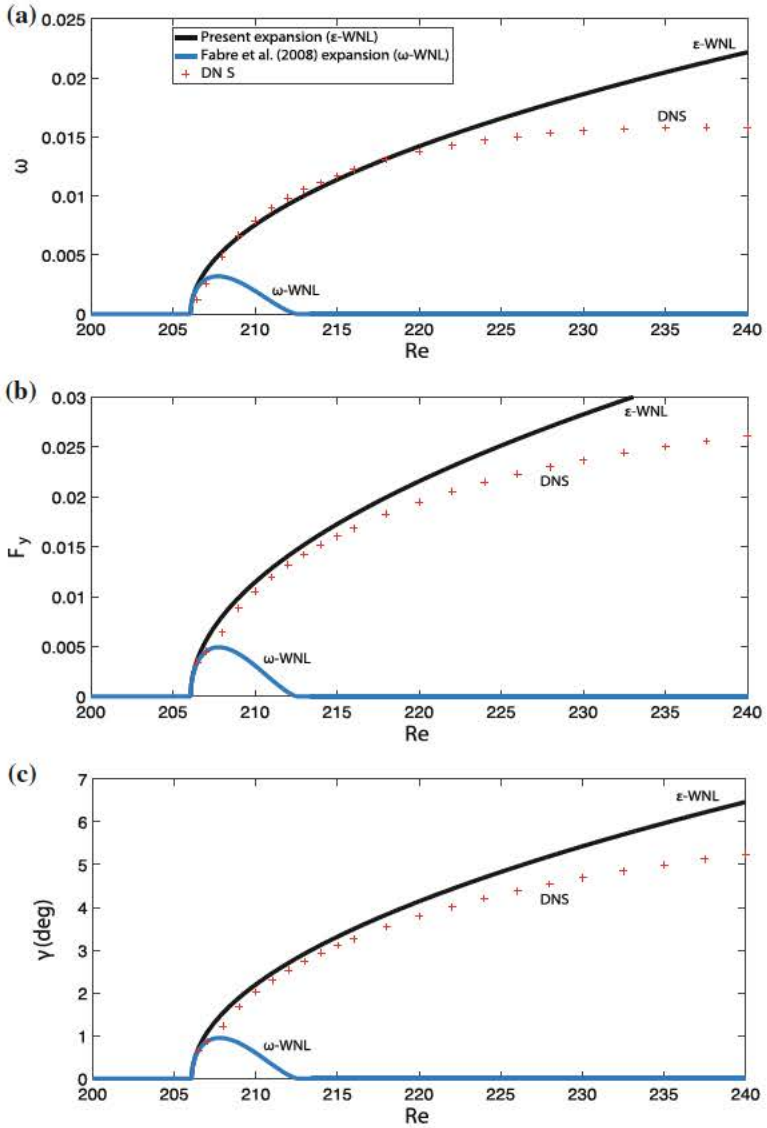

Fig. 3 Zero-torque solutions of a sphere. Comparison between DNS (*symbols*), ω-asymptotic expansion (*blue line*), ϵ-asymptotic expansion (*black line*). **a** Angular velocity; **b** lift force as a function of the Reynolds number; **c** slope angle γ, i.e., the angle between the lift force and the incoming flow

of a sphere in free fall and corresponds to the oblique, steady (OS) path observed in both experiments and simulations. A quantitative comparison against the data showed in Uhlmann and Dusek [10] was provided to support this.

To conclude, we shall address two interesting points which require some discussion. First, we stress again that, although the problem is characterized by two non-dimensional parameters, namely Re and the density ratio $\bar{\rho} = \rho_s/\rho_f$, all results presented here are actually independent upon this latter parameter. The fact that the steady solution computed by DNS or by the time-independent solution of the amplitude equation (5) does not depend upon the mass of the sphere is actually not so surprising, since the parameter $\bar{\rho}$ is only present in the term involving the angular acceleration (left-hand side of Eq. 1c). Hence, once the equilibrium is reached, inertia of the sphere does not enter into play any longer. It is more puzzling to note that the parameters σ and μ appearing in the amplitude equation (5) are also independent upon the mass. Therefore, in the vicinity of the threshold, not only the properties of the final state will be independent upon the mass, but also the transient dynamics experienced to reach it. This is somewhat counterintuitive, as one would expect that for a heavy sphere the transients will be longer than for a light sphere. A complementary study, considering the limit of very heavy objects (where a quasi-static approach is possible), is underway to explain this apparent paradox.

Secondly, the issue of secondary instability of the steady solution considered here is an open question to be addressed in future studies. In effect, the ability of the sphere to rotate (or to both rotate and translate) is expected to have an effect on the Hopf bifurcation which is known to occur in the range $Re \approx 270$. In the time-dependent states resulting from this secondary bifurcation, the angular velocity of the sphere will no longer be constant but will be given by the time-dependent solution of Eq. (1c). As a first step toward a rigorous study of this problem, we may look at the stability of the flow around a sphere rotating at exactly the angular velocity of the OS solution described above. This case actually constitutes a subset of a more general study conducted by [4], who gave a stability map in the $\omega - Re$ plane of the flow around a sphere rotating at a fixed, constant angular velocity. A more rigorous study of this problem, including the effect of the density ratio, is left for future studies.

References

1. Ern, P., Risso, F., Fabre, D., Magnaudet, J.: Wake-induced oscillatory paths of bodies freely rising or falling in fluids. Annu. Rev. Fluid Mech. **44**, 97–121 (2012)
2. Assemat, P., Fabre, D., Magnaudet, J.: The onset of unsteadiness of two-dimensional bodies falling or rising freely in a viscous fluid: a linear study. J. Fluid Mech. **690**, 173–202 (2012)
3. Auguste, F., Magnaudet, J., Fabre, D.: Falling styles of disks. J. Fluid Mech. **719**, 388–405 (2013)
4. Citro, V., Tchoufag, J., Fabre, D., Giannetti, F., Luchini, P.: Linear stability and weakly nonlinear analysis of the flow past rotating spheres. J. Fluid Mech (under review)
5. Johnson, T.A., Patel, V.C.: Flow past a sphere up to a Reynolds number of 300. J. Fluid Mech. **378**, 19–70 (1999)
6. Mordant, N., Pinton, J.F.: Velocity measurement of a settling sphere. Eur. Phys. J. B **18**, 343–352 (2000)
7. Horowitz, M., Williamson, C.H.K.: The effect of Reynolds number on the dynamics and wakes of freely rising and falling spheres. J. Fluid Mech. **651**, 251–294 (2010)
8. Obligado, M., Machicoane, N., Chouippe, A., Volk, R., Uhlmann, M., Bourgoin, M.: Path instability on a sphere towed at constant speed. J. Fluids Struct. **58**, 99–108 (2015)
9. Jenny, M., Dusek, J., Bouchet, G.: Instabilities and transition of a sphere falling or ascending freely in a Newtonian fluid. J. Fluid Mech. **508**, 201–239 (2004)
10. Uhlmann, M., Dusek, J.: The motion of a single heavy sphere in ambient fluid: a benchmark for interface-resolved particulate flow simulations with significant relative velocities. Int. J. Multiph. Flow **59**, 221–243 (2014)
11. Fabre, D., Tchoufag, J., Magnaudet, J.: The steady oblique path of buoyancy-driven disks and spheres. J. Fluid Mech. **707**, 24–36 (2012)
12. Tchoufag, J., Fabre, D., Magnaudet, J.: Weakly nonlinear model with exact coefficients for the fluttering and spiraling motion of buoyancy-driven bodies. Phys. Rev. Lett. **115**, 114501 (2015)
13. Citro, V., Giannetti, F., Luchini, P., Auteri, F.: Global stability and sensitivity analysis of boundary-layer flows past a hemispherical roughness element. Phys. Fluids **27**, 084110 (2015)
14. Tammisola, O., Giannetti, F., Citro, V., Juniper, M.: Second-order perturbation of global modes and implications for spanwise wavy actuation. J. Fluid Mech. **755**, 314–335 (2014)
15. Lashgari, I., Tammisola, O., Citro, V., Juniper, M., Brandt, L.: The planar X-junction flow: stability analysis and control. J. Fluid Mech. **753**, 1–28 (2014)
16. Sipp, D., Lebedev, A.: Global stability of base and mean-flows: a general approach and its applications to cylinder and open cavity flows. J. Fluid Mech. **593**, 333–358 (2007)
17. Meliga, P., Chomaz, J.M., Sipp, D.: Global mode interaction and pattern selection in the wake of a disk: a weakly nonlinear expansion. J. Fluid Mech. **633**, 159–189 (2009)
18. Hecht, F.: New development in FreeFem++. J. Numer. Math. **20**, 251–265 (2012)
19. Tchoufag, J., Fabre, D., Magnaudet, J.: Global linear stability analysis of the wake and path of buoyancy-driven disks and thin cylinders. J. Fluid Mech. **740**, 278–311 (2014)
20. Fabre, D., Auguste, F., Magnaudet, J.: Bifurcations and symmetry breakings in the wake of axisymmetric bodies. Phys. Fluids **20**(5), 051702 (2008)